Influence of cooling and reheating on the evolution of copper rich liquid in high residual low carbon steels

B. A. Webler*[1], E.-M. Nick[1], R. O'Malley[2] and S. Sridhar[1]

This study investigates some effects of austenite microstructure on processes leading to copper hot shortness. Low carbon steels containing 0·55 wt-% copper were subjected to two thermal profiles in an infrared image furnace with attached confocal scanning laser microscope: hold at 1150°C for 60 s; hold at 1150°C for 60 s, quench to 400°C, reheat to 1150°C. Heat treatments were conducted in dried/deoxidised argon to image microstructures. Subsequent samples were oxidised in air. The oxide/metal interface was studied in a scanning electron microscope. Additional confocal scanning laser microscope experiments involved melting copper directly on the steel. After quench/reheat, austenite grain size decreased by a factor of ~1·7 and grain boundaries were redistributed. Copper evolved during the first heating was no longer found at boundaries. Results from direct copper exposure reveal an apparent effect of boundary character on copper penetration rate. Possible mechanisms by which hot shortness is affected are discussed.

Keywords: High residual containing steels, Copper, Surface hot shortness, Phase transformation

Introduction

The use of recycled scrap in the production of low carbon steels in the electric arc furnace often introduces undesirable residual elements. One of these undesirable elements is copper because it is nobler than iron and enriches at the oxide/metal interface as the iron oxidises during casting, reheating and hot rolling. Copper has limited solubility in solid iron[1] and the new phase that separates is liquid at temperatures commonly encountered during steel production. The liquid wets and thereby embrittles the austenite grain boundaries, promoting intergranular surface cracking during hot deformation.[2] This phenomenon is known in the steel industry as 'copper induced surface hot shortness'. Crack formation in iron in the presence of liquid copper is often classified as an example of liquid metal embrittlement.[3]

Since good surface quality is an important goal for steel producers, significant attention has been focused on reducing or eliminating hot shortness by controlling reheat furnace conditions or steel chemistry. It is generally accepted that in the reheat furnace, low oxygen levels, low water vapour levels, and limitations on the time steel is exposed to temperatures between 1100 and 1250°C reduce hot shortness.[4] The maximum hot shortness severity is also dependent on the residual element content. The presence of tin lowers the solubility of copper in iron, exacerbating hot shortness.[2,5] Conversely, nickel reduces hot shortness by increasing the solubility of copper in iron.[6,7] Complete prevention of a copper rich liquid requires twice as much nickel as copper,[8] making it unfeasible as an industrial remedy. However, substantially smaller nickel additions can ameliorate hot shortness by promoting a phenomenon known as 'occlusion'.[9] This phenomenon involves metal enriched in copper and nickel to become incorporated in the iron oxide layer.

Much of the prior work on hot shortness focuses on connections between steel oxidation behaviour, the separated copper rich liquid, and material occluded into the oxide. Since the actual cause of hot shortness cracking is the penetration of liquid copper down austenite grain boundaries, the underlying austenite microstructure should play an important role in hot shortness. Specifically, the microstructure changes that occur in steel after casting may influence the behaviour of the copper rich liquid. Effects of austenite microstructure on copper induced surface hot shortness have not been widely investigated, likely since austenite microstructure in low carbon steel must be studied at high temperature.

In this work, the authors investigate some of the effects of modifying the austenite microstructure on the distribution of copper rich liquid, the main cause of surface hot shortness. Changes in the austenite microstructure were made by quenching to cause an austenite–ferrite transformation and subsequent reheating to produce new austenite. Heat treatments were conducted in a confocal scanning laser microscope (CSLM) with an

[1]Center for Iron and Steelmaking Research, Department of Materials Science and Engineering, Carnegie Mellon University, Pittsburgh, PA 15213, USA
[2]Nucor Steel Decatur LLC, 4301 Iverson Blvd., Trinity, AL 35673, USA

*Corresponding author, email bwebler@cmu.edu

Published by Maney on behalf of the Institute
Received 27 July 2007; accepted 4 April 2008
DOI 10.1179/174328108X318347

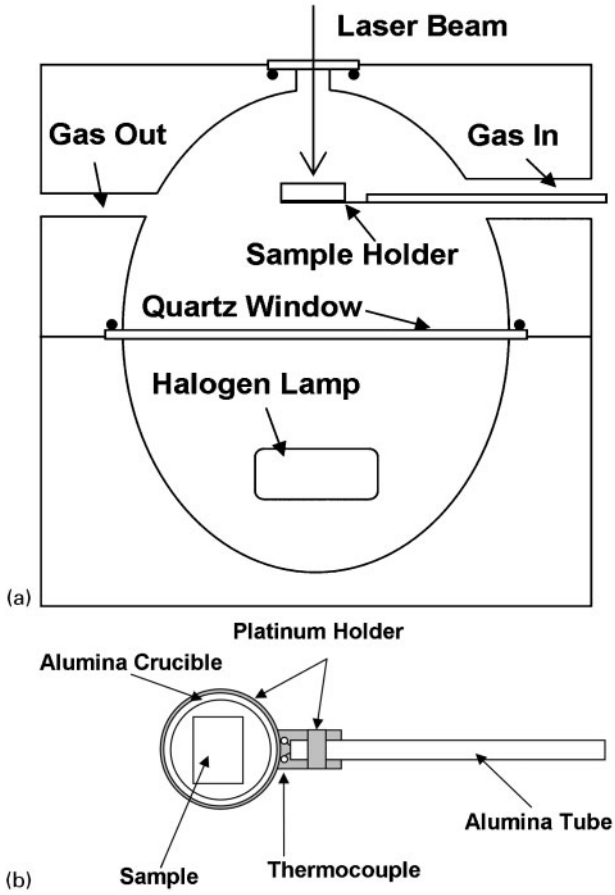

1 Schematic of CSLM set-up showing *a* high temperature furnace unit and *b* sample holder

attached high temperature furnace. This experimental set-up allows for some aspects of the austenite microstructure to be observed *in situ*. Introduction of the phase transformation has several effects on the distribution of copper rich liquid that can potentially reduce surface hot shortness.

Materials and methods

Materials

Low carbon steel containing copper and nickel was used for all experiments in this study. Significant hot shortness cracking would be expected in this sample at temperatures >1100°C.[10] The chemical composition of the sample used in this study is 0·128C–0·143Si–0·54Mn–0·55Cu–0·109Ni–0·016Sn–0·053S–0·011P (wt-%). This steel was industrially produced and supplied as hot rolled sheet.

Methods

The effect of heating and cooling on austenite microstructure and decomposition were investigated using a CSLM equipped for high temperature observation. A schematic of the furnace chamber and sample holder is shown in Fig. 1. The furnace chamber is an ellipsoid, so light from the halogen lamp (placed at one focus of the ellipsoid) reflects off the gold plated walls and focuses on the sample (placed at the other focus of the ellipsoid). This furnace set-up can achieve high heating and cooling rates. The microscope is equipped with a helium laser light source and confocal optics that permit direct visualisation of material at high temperatures. More information on the set-up and use of this microscope can be found in work by Sauerhammer *et al.*,[11] McDonald,[12] Chikama *et al.*,[13] and references therein.

Three types of experiments were performed in the CSLM:

(i) isothermal anneal used to compare with treatment (2) (Fig. 2*a*)
(ii) isothermal anneal with quench and reheat used to modify austenite microstructure (Fig. 2*b*)
(iii) longer time isothermal anneal with quench and reheat used to observe the effect of austenite microstructure on surface distribution of copper, described in detail below (Fig. 2*c*).

The experiments that were performed are listed in Table 1. For (i) and (ii), the entire heat treatment cycles were conducted first in argon gas to observe the

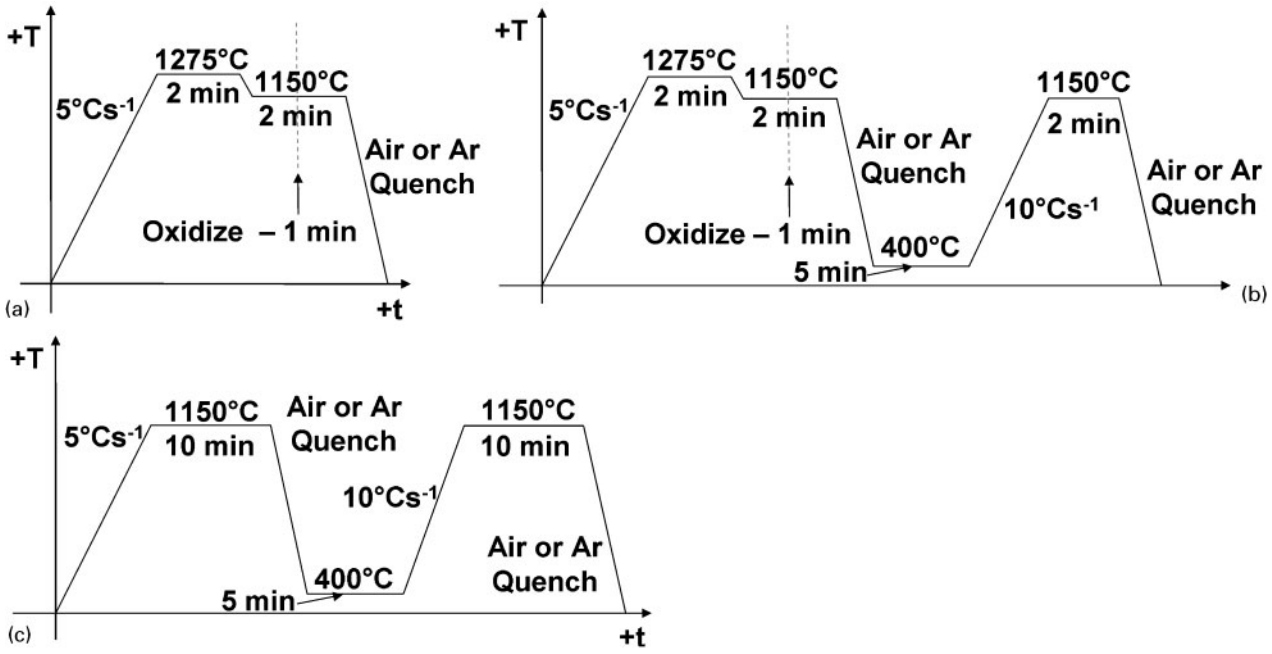

2 Schematic of heat treatments used in this study

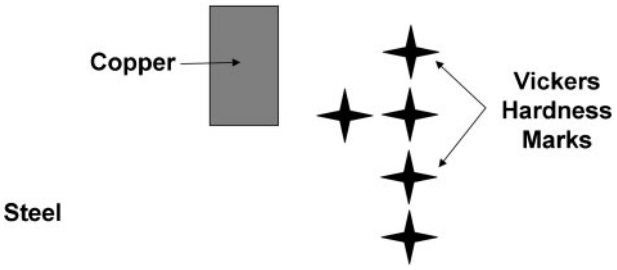

3 Schematic of sample 5, used for heat treatment in Fig. 2*c*: Vickers hardness marks were used to identify same area of surface in CSLM and in SEM

austenite microstructure and then repeated in air with a new sample to produce oxidised samples for microstructure characterisation. An initial heating to 1275°C for heat treatments (i) and (ii) (always conducted in argon regardless of whether the sample was to be oxidised) was used to grow the initial austenite grains to a size where the surface features could be easily studied. For (iii), a small piece of copper was placed on top of the sample and allowed to melt. Vickers hardness marks were used to identify the area viewed in the CSLM. The arrangement is shown schematically in Fig. 3. The 1275°C grain growth anneal was not used in heat treatment (iii).

The argon gas was purified by passing through a desiccant, heated copper turnings, and heated magnesium chips to remove any residual water vapour and oxygen. The air used was of unspecified purity but was passed through a desiccant to remove any residual water vapour.

After oxidation, the samples were mounted in a cold curing epoxy resin. The following vacuum impregnation procedure was used to preserve the interface structure: hold samples under vacuum, introduce the epoxy under vacuum, and finally slowly introduce air to force the epoxy into pores and gaps in the oxide. The samples were sectioned with a low speed diamond saw and polished to a 1 μm diamond finish. Some samples were etched in a 2% nital solution. All samples were coated with 2–2·5 nm of chromium or platinum to prevent charging in the SEM. Specific sample information is found in Table 1.

The SEM used was a Philips XL-20 SEM with a field emission gun source operating at 25 kV and a solid state backscattered detector installed. The working distance was 10 mm. Images were taken in secondary electron (SE) and backscattered electron (BSE) mode. Energy dispersive X-ray spectroscopy (EDS) was used to obtain qualitative compositional information. The open source software ImageJ[14] was used to measure grain perimeters of the austenite grains in the CLSM images.

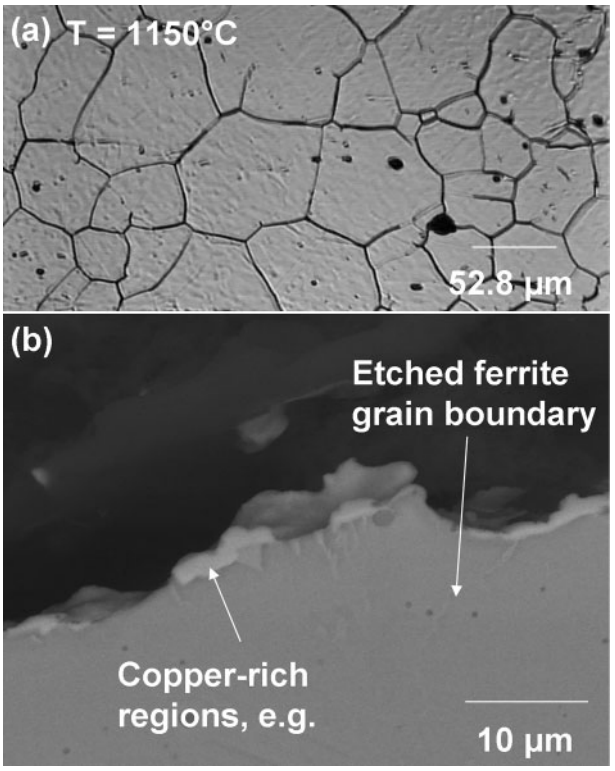

4 *a* CSLM image of sample 1 showing austenite grain structure and *b* BSE SEM image of sample 2 after isothermal oxidation for 60 s

Results

Isothermal oxidation

The austenite grain structure of sample 1 is shown in the CSLM image in Fig. 4*a*. The solid lines in Fig. 4*a* are due to thermal grooves formed by austenite grain boundaries intersecting the metal surface.[15] The austenite grain structure of sample 2, which was oxidised for 60 s, should be nearly identical to that shown in Fig. 4*a*. Oxidation of sample 2 for 60 s produced significant copper rich phase formation as shown in Fig. 4*b*. The indicated areas in the BSE SEM image are rich in copper, nickel and tin.

Isothermal oxidation plus phase transformation

The austenite–ferrite–austenite transformation was viewed directly with sample 3 during the heat treatment described in Fig. 2*b*. This sequence of transformation will be referred to as the '$\gamma/\alpha/\gamma$ transformation'. Images (CSLM) of sample 3 surface before the quench, after the quench, and after the reheating step are shown in Figs. 5*a–c* respectively. The broken lines in Fig. 5 represent austenite boundaries formed during the first heating step. These will be referred to as 'old' austenite boundaries. The quench rate used was rapid enough to produce Widmanstätten ferrite and the surface relief

Table 1 Individual sample identification and heat treatment information

Sample no.	Figure describing heat treatment	Atmosphere	Etching
1	Fig. 2*a*	Completely inert	None (CSLM sample only)
2	Fig. 2*a*	Air where indicated	2% nital solution
3	Fig. 2*b*	Completely inert	None (CSLM sample only)
4	Fig. 2*b*	Air where indicated	2% nital solution
5	Fig. 2*c*	Completely inert	None

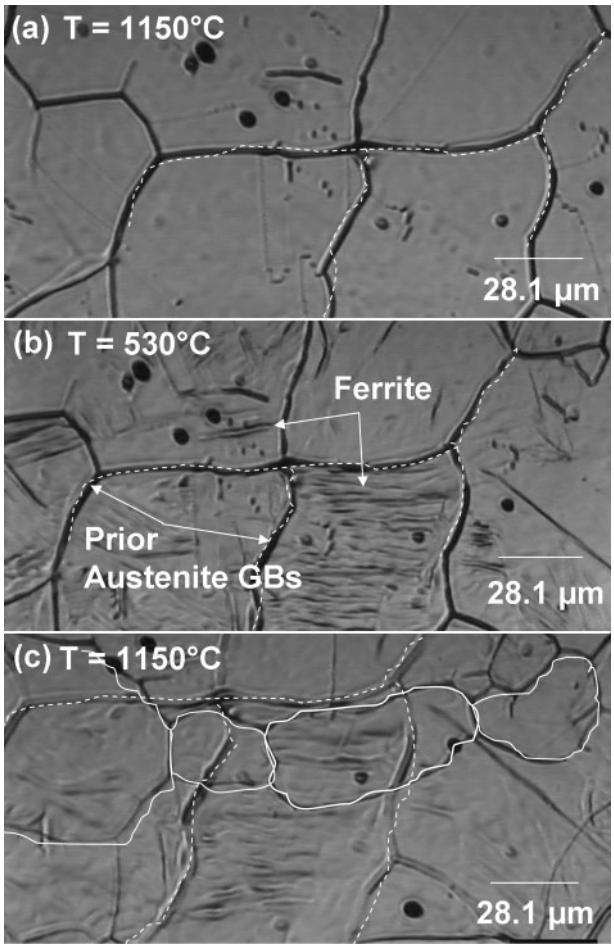

5 Images (CSLM) of sample 3 showing *a* austenite grain structure formed during first heating step (broken lines), *b* ferrite structure formed during quench and *c* austenite grain structure formed after second heating step (solid lines)

produced during the transformation[16] is indicated in the CSLM image in Fig. 5*b*. Figure 5*c* shows the formation of austenite grain boundaries upon reheating. These are indicated by the solid lines in Fig. 5*c* and will be referred to as 'new' austenite boundaries. Qualitatively, a decrease in austenite grain size can be discerned comparing Fig. 5*a* and *c*. Austenite grain perimeters were measured on a succession of CSLM images and it was found that the 'new' austenite grain perimeters decreased by $\sim$100 μm, a factor of 1·7 smaller than the 'old' austenite grain perimeters.

It can also be seen from Fig. 5*c* that the 'new' austenite grain boundaries do not correlate with the 'old' austenite boundaries. Figure 6 shows a site in a nital etched cross-section of sample 4 where this change in austenite boundary structure affected copper rich liquid that penetrated into the steel. Sample 4 was subjected to the same thermal history as sample 3 but under oxidising conditions. Measurements of EDS confirm that presence of copper is limited to the indicated area and that the other contrast is due to etched ferrite grain boundaries.

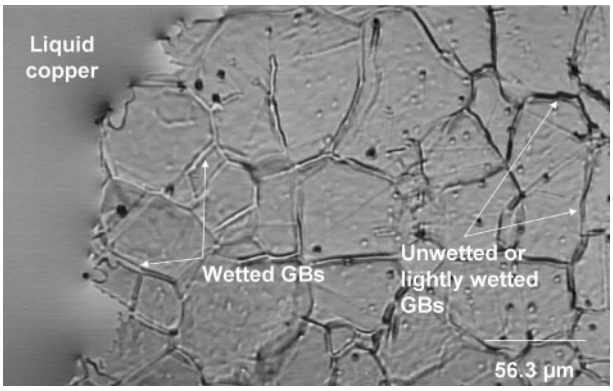

7 Image (CSLM) of sample 5 at 1150°C indicating that some differences can be observed between heavily wetted austenite grain boundaries and lightly wetted or unwetted austenite boundaries

Wetting behaviour of new grain boundaries

To investigate the wetting behaviour of 'new' and 'old' austenite grain boundaries, the same areas of sample 5 were observed in the CSLM and SEM by the procedure described above (see Fig. 3). Figure 7 shows a typical CSLM image of the surface at 1150°C. Austenite boundaries can be identified even in the presence of copper. Significant wetting of boundaries was observed

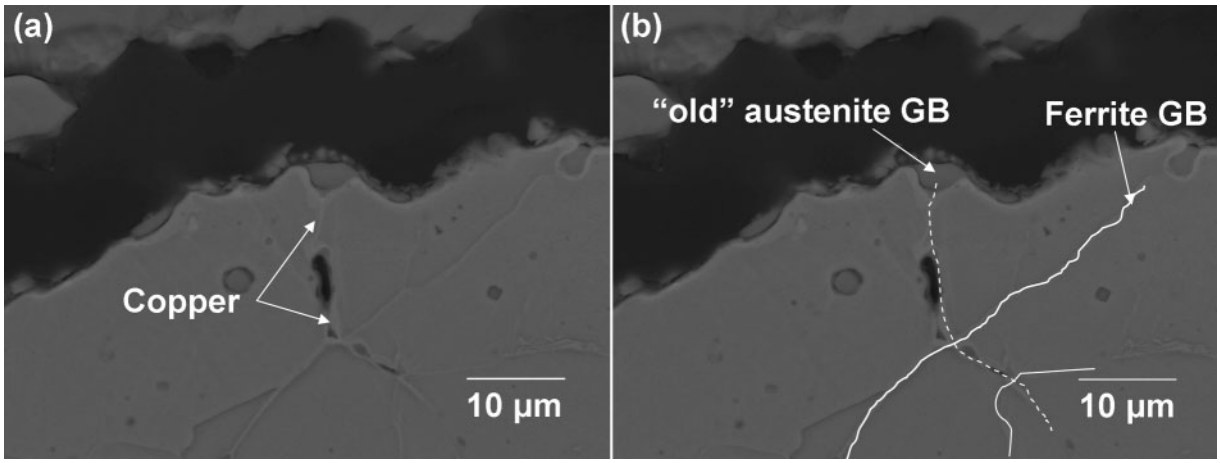

a original image; *b* traces out ferrite grain boundaries (solid lines) and 'old' austenite grain boundary (broken line)

6 Image (BSE SEM) of sample 4 showing copper penetration site (according to EDS measurements, copper is present only at 'old' austenite boundary)

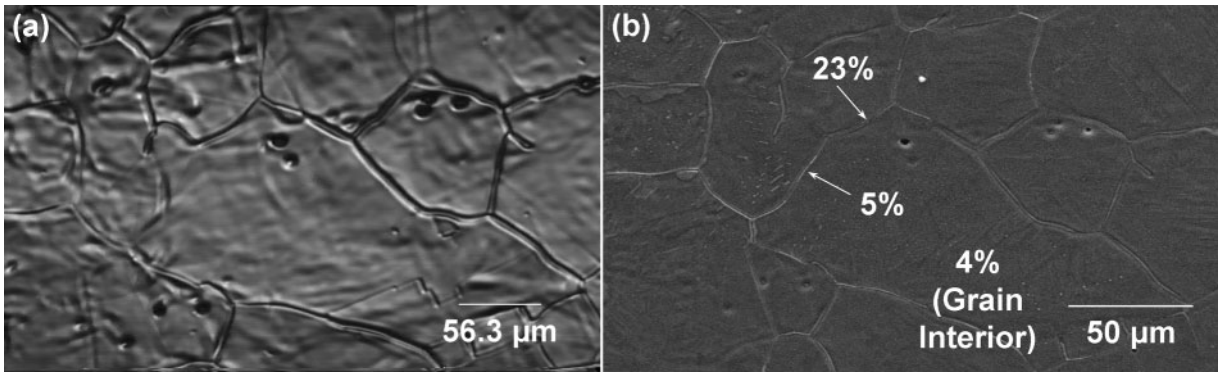

8 Images of same area of sample 5 from *a* CSLM at 1150°C and *b* SE SEM: numbers on SEM image refer to EDS measurements of copper content in wt-%

only near the liquid pool. Figure 8*a* shows a CSLM image just before quenching and Fig. 8*b* a secondary electron image of the same area. The numbers on Fig. 8*b* are EDS measurements of copper content in wt-%. The higher magnification image in Fig. 9 shows that different wetting behaviour was observed at different parts of a grain boundary. The effect is also seen at the triple points shown in Fig. 10.

Discussion

The results presented above demonstrate that the $\gamma/\alpha/\gamma$ transformation changes the austenite microstructure and affects processes related to surface hot shortness. The $\gamma/\alpha/\gamma$ transformation causes a decrease in grain size and a redistribution of austenite grain boundaries when comparing 'new' austenite boundaries to 'old' austenite boundaries. These changes in austenite microstructure can potentially have the following effects with respect to hot shortness:

(i) increased grain boundary diffusion of copper
(ii) increased toughness
(iii) shortened copper penetration depth
(iv) formation of new, copper free grain boundaries.

All of these effects should reduce hot shortness cracking.

The first major effect on austenite microstructure is a decrease in grain size, as shown comparing Fig. 5*a* and *c*. This relationship between grain size and the phase transformation is well known and is used to refine microstructure in normalising heat treatments.[17] The decrease in grain size (or increase in number of grain boundaries) should enhance copper diffusion back into the steel. If the quench rate could be improved, decreases in grain size could be obtained that are more significant than the factor of 1·7 measured in this work.

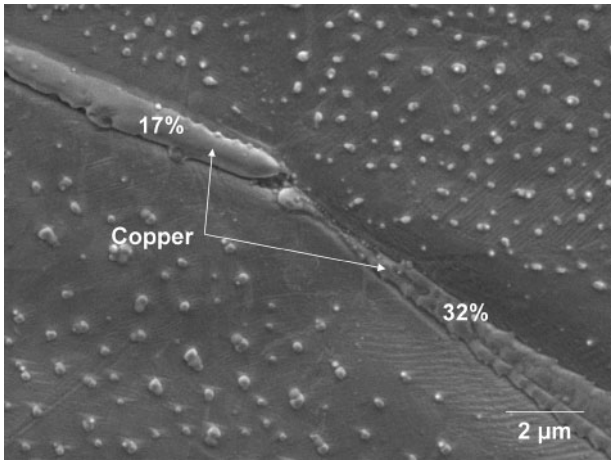

9 Image (SE SEM) of sample 5 showing changes in wetting behaviour along grain boundary: numbers refer to copper content measured by EDS (in wt-%); white particles are likely small iron oxide particles that form due to trace oxygen content in furnace gas

If these substantial decreases in grain size could be achieved, the increase in copper diffusivity can be easily estimated. According to a condition derived by Kaur and Gust,[18] diffusion fields normal to the grain boundary overlap if the grain size is smaller than $20(D_{LAT}\,t)^{1/2}$ with D_{LAT} representing the lattice diffusivity. If $D_{LAT}=2\times10^{-11}$ cm^2 s^{-1} (measured by Majima and Matani)[19] and $t=300$ s, grain sizes must be less than $\sim$15 μm for the above condition to hold. If this condition is met, diffusion in the system can be described by the effective diffusivity D_{EFF} (Ref. 18) which is defined as

$$D_{EFF}=D_{LAT}+\frac{4\delta D_{GB}}{3d} \quad (1)$$

where D_{LAT} is the lattice diffusivity, D_{GB} the grain boundary diffusivity, d the grain size and δ the grain boundary width. Apparent diffusivities for various grain sizes at 1150°C are shown in Table 2. Diffusivity can be increased nearly two orders of magnitude if the grain size is on the order of 1 μm. The increase in copper diffusivity will reduce the amount of liquid present at the oxide/metal interface.

In addition to enhancing diffusion, a decrease in grain size should also affect cracking behaviour. When liquid metal embrittlement occurs, failure is usually by intergranular fracture due to liquid metal present at grain boundaries.[3] The increased number of austenite grain boundaries should function as barriers to crack propagation, decreasing the severity of surface cracking.

Table 2 Grain size effect on copper diffusivity in iron calculated from equation (1): D_{LAT} and δD_{GB} numbers come from Majima and Matani[19]

D_{LAT}, cm ^{2}s^{-1}	$2{\cdot}65\times10^{-11}$
δD_{GB}, cm ^{3}s^{-1}	$2{\cdot}96\times10^{-13}$
d, μm	D_{EFF}, cm^2 s^{-1}
1	$2{\cdot}98\times10^{-9}$
10	$3{\cdot}22\times10^{-10}$
50	$8{\cdot}57\times10^{-11}$

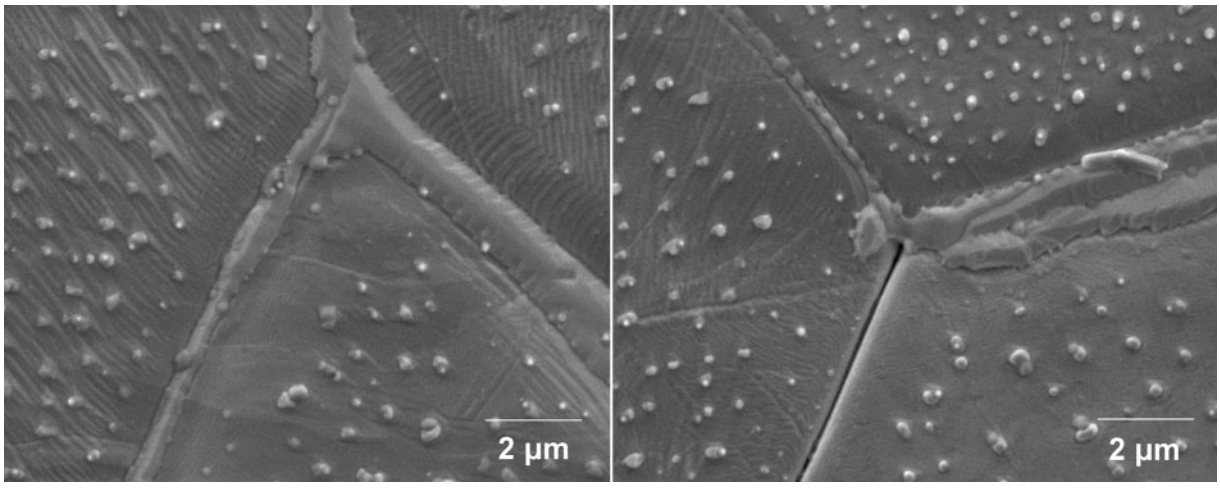

10 Image (SE SEM) of sample 5 showing changes in wetting behaviour at two different triple points

Beneficial effects of small grain size have been previously observed in low carbon steel embrittled by liquid lithium.[20] In terms of embrittlement of steel by copper, Shibata *et al.*[10] observed that smaller grain sizes were beneficial, though they did not report grain size measurements. It is expected that faster quench rates, leading to smaller austenite grains on reheating, would enhance the above mentioned effects.

The $\gamma/\alpha/\gamma$ transformation also changes the distribution of austenite grain boundaries, as shown in Fig. 5. The BSE SEM image of sample 4 in Fig. 6 shows a region where copper has penetrated into the steel, though it is not apparent whether it lies at an 'old' or 'new' austenite grain boundary. However, consideration of the surrounding microstructure suggests that the copper lies at an 'old' boundary. The nital etch reveals a ferrite grain boundary passing directly through the penetrated region. This boundary and the copper rich penetration are traced out in Fig. 6*b* (solid line=ferrite grain boundaries, broken line=copper rich phase). If the assumption is made for the moment that the observed copper penetration lies at a 'new' austenite boundary, any ferrite grains forming on the final quench would have grown perpendicular to copper penetration (since ferrite nucleates at austenite grain boundaries). It is not likely that the ferrite would grow in such a manner that it crosses the austenite boundary from which it nucleated. It is more likely that the ferrite formed at a 'new' austenite boundary at some other point in the sample (which can be no longer observed due to the transformation on cooling) and the copper penetration thus lies on an 'old' austenite boundary. Measurements of EDS confirm that presence of copper is limited to the penetration and that the other contrast is due to etched ferrite grain boundaries.

The schematic in Fig. 11 shows the effect of this change on copper. Liquid copper formed up to the point of transformation lies at the oxide/metal interface and at austenite grain boundaries (Fig. 11*a*). After the $\gamma/\alpha/\gamma$ transformation, the original copper penetrations no longer lie at austenite grain boundaries (Fig. 11*b*). Any cracking caused by this copper would be transgranular and likely more difficult to propagate through the material than intergranular cracks.

Eventually, copper will be found at the 'new' austenite grain boundaries. The most likely source of copper is that produced by oxidation after the $\gamma/\alpha/\gamma$ transformation, but observations in this work suggest that 'new' austenite boundaries can be wet by copper from the 'old' austenite boundaries. Figure 8*a* shows a CSLM image of the 'new' austenite structure for sample 5. Examination of the recorded experiment confirms that the boundaries shown in Fig. 8*a* and *b* are 'new' austenite boundaries and not remnants of 'old' wetted

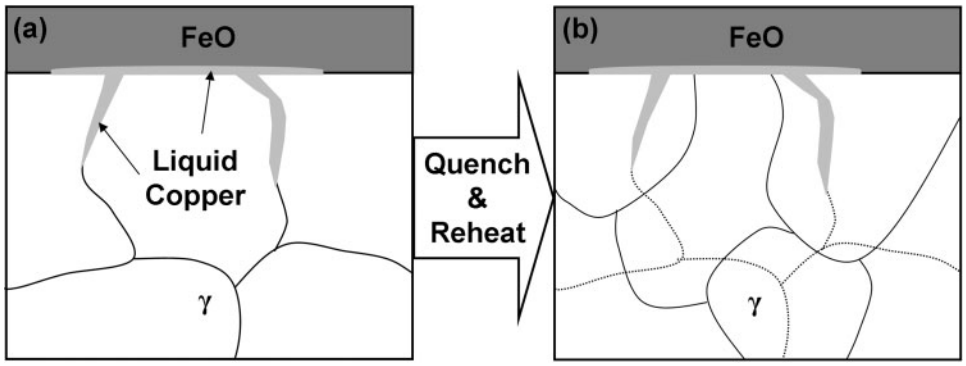

a case before quenching and reheating, where copper lies on austenite grain boundaries; *b* after boundaries are redistributed (after quenching and reheating), copper no longer lies along austenite grain boundaries (broken lines refer to 'old' austenite boundaries and solid lines to 'new' austenite boundaries)

11 Schematic showing effect of austenite boundary redistribution on copper penetrations formed before quenching and reheating

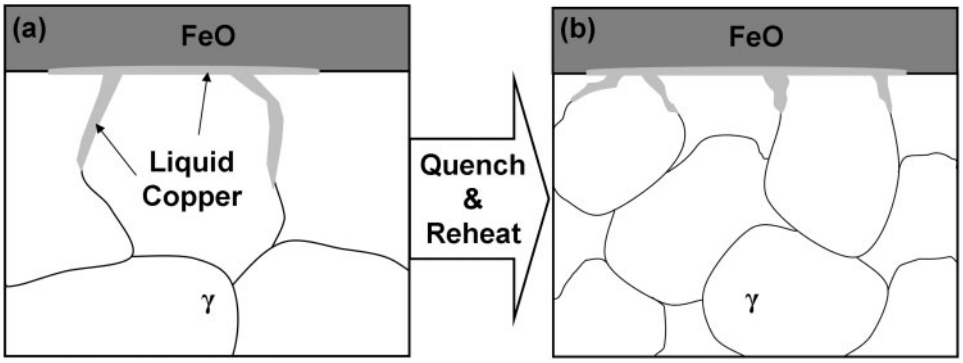

12 Schematic showing how *a* larger and *b* smaller austenite grain size (formed after quenching and reheating) affect penetration depth of liquid copper

austenite boundaries. Figure 8*b* shows an SE SEM image of the same area as the CSLM image. The EDS measurements show copper present at the 'new' grain boundaries, but the amount varies depending on position. The EDS measurements of copper content taken at points away from boundaries were usually lower than measurements taken at the grain boundaries. This suggests that the copper present at the 'old' austenite grain boundaries has migrated, either by diffusion or bulk flow, to the 'new' grain boundaries. If this were not the case, i.e. copper remained at the 'old' boundaries, significant copper concentrations would be expected in the interior of the 'new' austenite grains (where the 'old' austenite boundaries once were), and none were observed.

Not all of the copper in these 'new' boundaries came from the 'old' boundaries, however. Another likely source was copper from the liquid pool transported either by bulk flow of the liquid or surface diffusion. No bulk flow of copper from the liquid pool to the grain boundaries was observed in the CSLM, but significant surface diffusion likely occurred. Exact surface diffusion data for this problem is unavailable, so an order of magnitude estimate of the surface diffusivity was used based on numbers for nickel.[21] A surface diffusivity of $\sim 10^{-5}$ cm^2 s^{-1} suggests that surface diffusion is rapid enough to transport copper from the liquid pool to the observed area which was 150 μm away. The copper observed at the 'new' boundaries likely came from both surface diffusion from the original pool and copper at the 'old' boundaries.

In real steels, whether copper at 'new' austenite boundaries came from oxidation or from 'old' boundaries, the increased number of grain boundaries should provide more places for copper to penetrate into the steel. Instead of isolated and deep copper penetrations, frequent and shallow copper penetrations should result. This mechanism is similar to that proposed by Shibata[10] and Fig. 12 shows comparison before and after quench/reheat (i.e. larger (Fig. 12*a*) and smaller (Fig. 12*b*) austenite grains). When testing the creep properties of iron in the presence of liquid copper, Hough and Rolls[22] determined that the growth rate of surface cracks was determined by the depth of copper penetration. Thus shallower penetration depths result in less copper present at each boundary and therefore a reduction in crack depth.

Close inspection of the surface in the SEM also revealed changes in wetting behaviour at surface grain boundaries. Examples of these phenomena are shown in Figs. 8 and 9. These results provide reasonable confirmation that actual wetting of the surface austenite grain boundaries occurred rather than simply flow of the liquid copper down a channel formed by the grain boundary groove. Since different boundaries are wetted to different degrees, grain boundary character must play a role in copper wetting. A slightly modified version of the wetting problem was studied by Wynblatt *et al.*,[23] using an iron manganese copper alloy with high enough copper concentration to form a second, copper rich phase. The manganese was used to stabilise austenite to room temperature, where correlations were made between wetting of the copper rich phase and grain boundary character. Different grain boundaries were found to have different wetting behavior. This experimental set-up does not exactly correlate with the common hot shortness situation, i.e. a liquid copper film penetrating into iron grain boundaries and therefore the results may not be directly applicable to the current study. However, upon exposing pure iron to liquid copper, Savage[24] and Fredriksson[25] observed liquid copper at a significant number of boundaries and both studies observed that the depth of copper penetration increased with time. Considering these results and those observed in the present study, it appears that the austenite grain boundary character affects both wetting behaviour and the rate at which copper penetrates down the grain boundaries.

Conclusions

1. Application of an austenite to ferrite to austenite transformation decreases the austenite grain size formed during the second heating step. It also changes the distribution of austenite grain boundaries. These changes can potentially affect surface hot shortness caused by liquid copper penetration.

2. The decreased austenite grain size after transformation promotes diffusion of copper back into the steel and reduces the amount of liquid copper available. It also increases the number of places where copper can penetrate; short, frequent penetrations are created instead of deep penetrations. Shorter crack lengths have been associated with shorter penetrations.

3. Redistribution of the austenite grain boundaries after the transformation creates areas where copper rich liquid no longer lies at austenite grain boundaries.

4. Different grain boundaries on the steel surface have different wetting behaviour. Some surface grain boundaries have no copper present for experimental times studied.

Acknowledgement

Financial support from the Center for Iron and Steelmaking Research (CISR) and the Pennsylvania Infrastructure Technology Alliance (PITA) is gratefully acknowledged.

References

1. L. J. Schwartzendruber: in 'Phase diagrams of binary copper alloys', (ed. P. R. Subramanian *et al.*), 1st edn, 167–172; 1994, Materials Park, OH, ASM International.
2. D. A. Melford: *J. Iron Steel Inst.*, 1962, **200**, 290.
3. M. G. Nicholas and C. F. Old: *J. Mater. Sci.*, 1979, **14**, 1–18.
4. A. Nicholson and J. D. Murray: *J. Iron Steel Inst.*, 1965, **203**, 1007.
5. N. Imai, N. Komatsubara and K. Kunishige: *ISIJ Int.*, 1997, **37**, 217–223.
6. N. Imai, N. Komatsubara and K. Kunishige: *ISIJ Int.*, 1997, **37**, 224–231.
7. W. J. M. Salter: *J. Iron Steel Inst.*, 1966, **204**, 478.
8. G. G. Foster and J. K. Gilchrist: *Metallurgia*, 1952, **225**, 225.
9. G. L. Fisher: *J. Iron Steel Inst.*, 1969, **207**, 1010.
10. K. Shibata, S.-J. Seo, M. Kaga, H. Uchino, A. Sasanuma, K. Asakura and C. Nagasaki: *Mater. Trans. JIM*, 2002, **43**, 292–300.
11. B. Sauerhammer, D. Senk, E. Schmidt, M. Safi, M. Spiegel and S. Sridhar: *Metall. Mater. Trans. B*, 2005, **36B**, 503–512.
12. N. McDonald: 'Peritectic solidification in ferrous alloys', PhD thesis, Carnegie Mellon University, Pittsburgh, PA, USA, 2004.
13. H. Chikama, H. Shibata, T. Emi and M. Suzuki: *Mater. Trans. JIM*, 1996, **37**, 620–626.
14. W. Rasband: *ImageJ*, Windows v. 1·36, available at: http://rsb.info.nih.gov/ij/ (accessed 20 August 2006).
15. W. W. Mullins: *J. Appl. Phys.*, 1957, **28**, 333–339.
16. J. W. Christian: in 'Decomposition of austenite by diffusional processes', (ed. V. F. Zackay and H. I. Aaronson), 371–386; 1962, New York, Wiley.
17. B. Liščić: in 'Steel heat treatment handbook', (ed. G. E. Trotten and M. A. H. Howes), 1st edn, 527–662; 1997, New York, Marcel Dekker, Inc.
18. I. Kaur and W. Gust: 'Fundamentals of grain and interphase boundary diffusion', 77–90; 1989, Stuttgart, Ziegler Press.
19. K. Majima and H. Mitani: *Trans. Jpn Inst. Met.*, 1978, **19**, 663–668.
20. E. G. Coleman, D. Weinstein and W. Rostoker: *Acta Metall.*, 1961, **9**, 491–496.
21. P. Shewmon: 'Diffusion in solids', 217; 1989, Warrendale, PA, The Minerals, Metals & Materials Society.
22. R. R. Hough and R. Rolls: *J. Mater. Sci.*, 1971, **6**, 1493–1498.
23. P. Wynblatt and M. Takashima: *Interf. Sci.*, 2001, **9**, 265–273.
24. W. F. Savage, E. F. Nippes and R. P. Stanton: *Weld. Res. Suppl.*, 1978, **57**, 9s–16s.
25. H. Fredriksson, K. Hansson and A. Olsson: *Scand. J. Metall.*, 2001, **30**, 41–50.